CrossMark

Synthesis, Structural Characterization, Theoretical Calculations and In Vitro Biological Activities of Organotin(IV) Complexes with [O,O] Donor Ligand

Fatima Javed[1] · Saqib Ali[1] · Saira Shahzadi[1] · Saroj K. Sharma[2] · Kushal Qanungo[2] ·
Muhammad Nawaz Tahir[3] · Naseer Ali Shah[4] · Muhammad Rashid Khan[5] ·
Nasir Khalid[6]

Abstract The present study deals with the synthesis of ligand 4-oxo-4-(thiazol-2-ylamino)butanoic acid and afterward its organotin(IV) carboxylates [Bu$_3$SnL] (**1**), [Ph$_3$SnL] (**2**), [Me$_2$SnL$_2$] (**3**), [Bu$_2$SnL$_2$] (**4**) and [Ph$_2$SnL$_2$] (**5**). These complexes were characterized by useful techniques like elemental analysis, FT-IR, NMR (^{1}H, ^{13}C) and single crystal analysis. The ligand coordinates to tin atom via the carboxylate group. Complex **1** has also been studied by single crystal XRD analysis. It showed that tin has distorted tetrahedral geometry due to bulky butyl groups that hinder the carbonyl oxygen of the ligand interaction with the adjacent tin atom for further coordination. The HOMO–LUMO study of ligand "**HL**" and its tin complexes **3** and **5** indicated that tin complexes are thermodynamically more stable than the ligand. The synthesized complexes were screened for their biological activities like antibacterial, antifungal, antileishminial, cytotoxicity and protein kinase inhibition studies in vitro. Complexes **1** and **2** exhibited maximum antileishmanial activity that was even higher than that of standard Amphotericin B, with significant cytotoxicity and could be potential candidates for the treatment of leishmaniasis. The UV–visible spectroscopic studies revealed that ligand and its complexes bind with DNA via intercalative mode of interaction leading to hypochromism and minor bathochromic or hypsochromic shifts.

1 Introduction

Organotin(IV) compounds of carboxylic acids are being extensively studied with special reference to their methods of synthesis, structural elucidation, and biological activities [1, 2]. Organotin compounds have some potential to be used as antitumor and anticancer drugs probably due to the dissociative nature of organotin(IV) moieties [3]. Biological activity is generally associated with the nature of organic ligand [4, 5] which facilitates the transportation of the complexes across the cell membrane. Spectroscopic characterization of organotin(IV) carboxylates confirmed the presence of great structural variety both in solid and solution states. Moreover the anionic ligands are highly effective for tin owing to the greater stability of the resulting metal carboxylates, which is attributed to the steric and electronic factors of organic substituent on the tin and/or the carboxylate moiety which impart significant resonance contribution to the overall electronic structure.

✉ Saqib Ali
 drsa54@yahoo.com; drsa54@hotmail.com

[1] Department of Chemistry, Quaid-i-Azam University, Islamabad 45320, Pakistan

[2] Department of Applied Sciences and Humanities, Faculty of Engineering and Technology, Mody Institute of Technology and Science (Deemed University), Lakshmangargh, Dist. Sikar 332311, Rajasthan, India

[3] Department of Physics, University of Sargodha, Sargodha, Pakistan

[4] Department of Biosciences, COMSATS Institute of Information Technology, Islamabad, Pakistan

[5] Department of Biochemistry, Quaid-i-Azam University, Islamabad 45320, Pakistan

[6] Chemistry Division, Pakistan Institute of Nuclear Science and Technology, P.O. Nilore, Islamabad, Pakistan

The carboxylate ligands can bind with the ionic tin center in different modes leading to monomeric, oligomeric (dimeric, tetrameric) ladders and hexagonal drum like structures [6–8]. For the synthesis of organotin(IV) carboxylates, a number of new synthetic techniques such as solvothermal synthesis and others are commonly employed, but conventional synthetic methods such as azeotropic dehydration or salt elimination methods are still in use [9].

The present study deals with the synthesis of di- and tri-organotin(IV) carboxylates of the type $R_{4-n}SnL_n$ (R = Me, Bu, Ph), L = 4-oxo-4-(thiazol-2-ylamino)butanoic acid and n = 1 or 2 employing reflux method. These compounds were characterized by elemental analysis, FT-IR, NMR (^{1}H and ^{13}C), semi-empirical and single crystal X-ray analysis. The potential of the synthesized complexes was tested for their antibacterial, antifungal, antileishminial, cytotoxic and protein kinase inhibition. DNA interaction studies of the synthesized complexes were also conducted.

2 Experimental

2.1 Materials and Methods

Reagents Bu$_3$SnCl, Ph$_3$SnCl, Me$_2$SnCl$_2$, Bu$_2$SnCl$_2$, Ph$_2$SnCl$_2$, 2-amino thiazol and succinic anhydride were obtained from Aldrich (USA) and were used without further purification. All the solvents purchased from E. Merck (Germany) were dried before use, according to the reported procedures [10]. Melting points were recorded with a Bio-Cote Model SMP10 melting point apparatus and are uncorrected. FT-IR spectra were recorded with a Thermo Scientific Nicolet-6700 FTIR spectrometer in the range 4000–250 cm^{-1}where as the NMR spectra were obtained

60.0 mm from the crystal. The crystals were cooled to 100 ± 1 K using the Bruker KRYOFLEX low temperature device and intensity measurements were performed using graphite monochromated Mo-Kα radiation from a sealed ceramic diffraction tube (SIEMENS). Generator settings were 50 kV/40 mA. The structure was solved by Patterson method and an extension of the model was accomplished by the direct method using the program DIRDIF or SIR2004. Final refinement on F2 was conducted by full matrix least squares techniques using SHELXL-97, a modified version of the program PLUTO (preparation of illustrations) and PLATON package.

2.2 Synthesis

2.2.1 Synthesis of Ligand (HL)

Solution of succinic anhydride (1 mmol) in toluene (100 mL) was mixed with a solution of 2-aminothiazol (1 mmol) in toluene (80 mL) in a 250 mL round bottom flask. The reaction mixture was magnetically stirred at room temperature for 24 h. The product was precipitated, filtered and washed with cold distilled water (400 mL) in order to remove unreacted precursors.

Yield: 90 %: M.p. 152–154 °C: Mol. Wt.: 200.03: elemental anaysis: % (calculated) for C$_7$H$_8$N$_2$O$_3$S: C, 41.99 (41.95); H, 4.03 (4.00); N, 13.99 (13.97); S, 16.02 (16.58): **IR** (4000–250 cm^{-1}): 3117ν (OH); 3346ν (NH); 1700ν (amide C=O); 1546ν (COO$_{asym}$); 1260ν (COO$_{sym}$); 286 (Δν); ^{1}**H NMR** (DMSO-d$_6$, 300 MHz) δ (ppm): 12.17 (bs, 1H, OH); 2.66 (m, 2H, H2); 2.55 (m, 2H, H3); 12.15 (bs, 1H NH); 7.44 (d, 1H, H6, ^3J[^{1}H, ^{1}H] = 3.6 Hz); 7.17 (d, 1H, H7, ^3J[^{1}H, ^{1}H] = 3.6 Hz): ^{13}**C NMR** (DMSO-d$_6$, 75 MHz) δ (ppm): 174.0 (C1); 30.2 (C2); 28.8 (C3); 170.6(C4); 158.4 (C5); 138.4 (C6); 113.6 (C7).
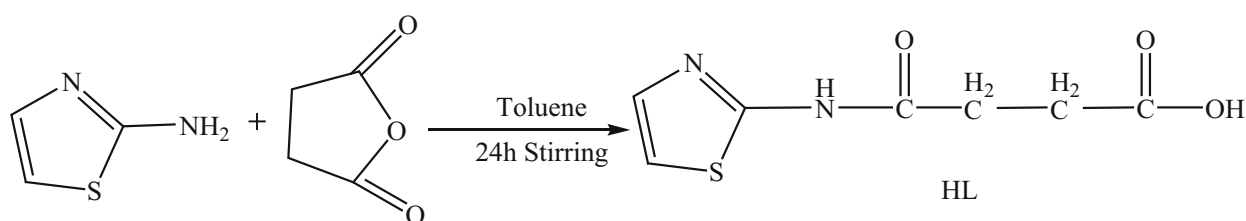
with BrukerAvance 300 MHz NMR spectrometer. Absorption spectra were measured on UV–Vis spectrometer, Shimadzu 1800 at ambient temperature of 25 ± 1 °C. Sodium salt of DNA (ACROS) was used as received. The quantitative determination of C, H, N and S was carried out using a LECO CHNS-932 analyzer. The X–ray diffraction data was collected on a Bruker SMART APEX CCD diffractometer, equipped with a 4 K CCD detector set

2.2.2 Synthesis of Sodium Salt of Ligand (NaL)

Equimolar aqueous solutions (5 mmol) of sodium hydrogen carbonate and ligand (**HL**) were taken in a 100 mL round bottom flask. The mixture was stirred at room temperature to get a clear solution, which was then rotary evaporated to yield a solid state of the desired sodium salt of the ligand.
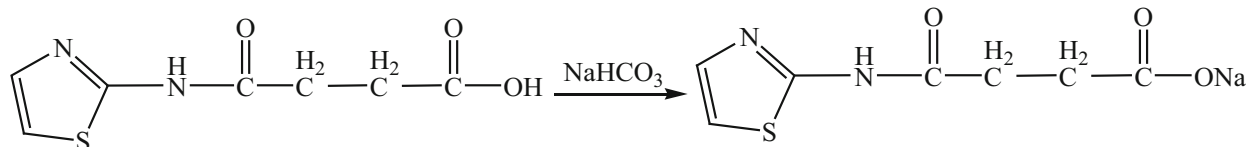
2.2.3 Synthesis of Organotin(IV) Complexes

Organotin(IV) carboxylate complexes were prepared by refluxing a mixture of sodium salt of ligand NaL (5 mmol) and R_3SnCl (5 mmol) or R_2SnCl_2 (2.5 mmol) in dry toluene for 8 h according to Scheme 1. The resultant refluxed solution was kept over night at room temperature. The precipitated NaCl, was filtered off and the solvent was evaporated under reduced pressure. Synthesized product was purified by recrystallization from chloroform at room temperature. The numbering scheme of **HL** and other organic moieties attached to tin atom for NMR interpretation is shown in Scheme 2.
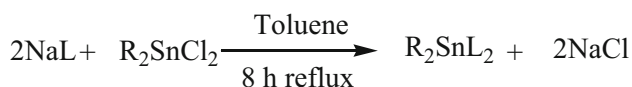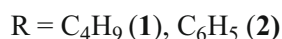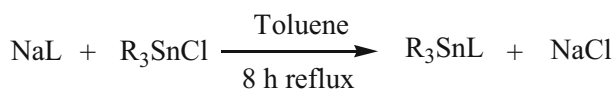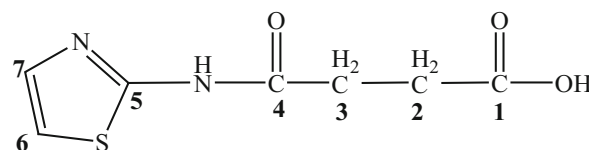
2.2.4 Tributylstannyl-4-oxo-(thiazol-2-ylamino)butanoate (1)

Yield: 81 %: M.p. 111–112 °C: Mol. Wt.: 490.13: elemental anaysis: % (calculated) for $C_{19}H_{34}N_2O_3SSn$: C, 46.64(46.62); H, 7.00 (6.97); N, 5.73 (5.71); S, 6.55 (6.52): **IR** (cm^{-1}): 3345 ν (NH); 1695 ν (amide C=O); 1563 ν (COO_{asym}); 1314 ν (COO_{sym}); 249 (Δν); 574 ν (Sn–C); 475 ν (Sn–O): **^{1}H NMR** (DMSO-d_6, 300 MHz) δ (ppm): 2.57 (t, 2H, H2, $^3J[^1H, {}^1H] = 7.2$); 2.38 (t, 2H, H3, $^3J[^1H, {}^1H] = 7.2$); 11.98 (bs, 1H, NH); 7.41 (d, 1H, H6, $^3J[^1H, {}^1H] = 3.6$ Hz); 7.13 (d, 1H, H7, $^3J[^1H, {}^1H] = 3.6$ Hz);1.52 (m, 6H,Hα); 1.24 (m, 6H, Hβ); 1.00 (m, 6H, Hγ); 0.83 (t,9H, Hδ, $^3J[^1H, {}^1H] = 7.2$ Hz): **^{13}C NMR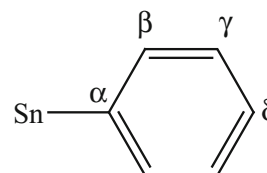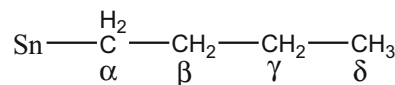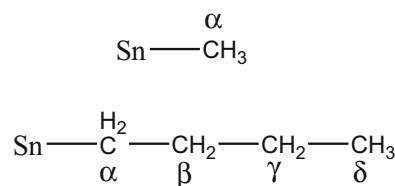** (DMSO-d_6, 75 MHz) δ (ppm): 175.9 (C1); 31.7 (C2); 30.2 (C3); 171.2 (C4); 158.6 (C5); 137.8 (C6); 113.3 (C7); 18.8 $(Cα, {}^1J[^{119/117}Sn-^{13}Cα] = 474, 456$ Hz); 28.0 $(Cβ, {}^2J[^{119}Sn-^{13}Cβ] = 27$ Hz); 26.9 $(Cγ, {}^3J[^{119/117}Sn-^{13}Cγ] = 77, 75$ Hz); 14.0 (Cδ).

2.2.5 Triphenylstannyl-4-oxo-(thiazol-2-ylamino)butanoate (2)

Yield: 84 %: M.p. 128–129 °C: Mol. Wt.: 550.04: elemental anaysis: % (calculated) for $C_{25}H_{22}N_2O_3SSn$: C, 54.67 (54.62); H, 4.04 (4.01); N, 5.10 (5.09); S, 5.84 (5.81): **IR** (4000-250 cm^{-1}): 3347 ν(NH); 1710 ν(amide C=O); 1514 ν(COO_{asym}); 1360 ν(COO_{sym}); 154 (Δν);277 ν (Sn–C); 479 ν (Sn–O): **^{1}H NMR** (DMSO-d_6, 300 MHz) δ (ppm): 2.55 (m, 2H, H2); 2.35 (t, 2H, H3, $^3J[^1H, {}^1H] = 7.2$); 12.10 (bs, 1H, NH); 7.44 (d, 1H, H6, $^3J[^1H, {}^1H] = 3.6$ Hz); 7.16 (d, 1H, H7, $^3J[^1H, {}^1H] = 3.6$ Hz); 7.88 (m, 6H, Hβ); 7.35 (m, 6H, Hγ); 7.26 (m, 3H, Hδ): **^{13}C NMR** (DMSO-d_6, 75 MHz) δ (ppm): 175.3 (C1); 31.8 (C2); 31.7 (C3); 171.4 (C4); 158.6 (C5); 128.5 (C6); 113.4 (C7); 137.9 $(Cα, {}^1J[^{119/117}Sn-^{13}Cα] = 636, 620$ Hz); 128.1 $(Cβ, {}^2J[^{119/117}Sn-^{13}Cβ] = 62, 59$ Hz); 136.8 $(Cγ, {}^3J[^{119}Sn-^{13}Cγ] = 48$ Hz); 126.0 (Cδ).

$$NaL + R_3SnCl \xrightarrow[\text{8 h reflux}]{\text{Toluene}} R_3SnL + NaCl$$

$$R = C_4H_9 (1), C_6H_5 (2)$$

$$2NaL + R_2SnCl_2 \xrightarrow[\text{8 h reflux}]{\text{Toluene}} R_2SnL_2 + 2NaCl$$

$$R = CH_3 (3), C_4H_9 (4), C_6H_5 (5)$$

Scheme 1 Chemical equations for synthesis of organotin(IV) complexes

Scheme 2 Numbering scheme of **HL** and other organic moieties attached to tin atom for NMR interpretation

2.2.6 Dimethylstannicbis[4-oxo-(thiazol-2-ylamino)]butanoate (3)

Yield: 75 %: M.p. 124–125 °C: Mol. Wt.: 547.98: elemental anaysis: % (calculated) for $C_{16}H_{20}N_4O_6S_2Sn$: C, 35.12 (35.08); H, 3.68 ((3.63); N, 10.24 (10.22); S, 11.72 (11.68): **IR** (4000–250 cm^{-1}): 3343 ν(NH); 1704 ν(amide C=O); 1556 ν(COO_{asym}); 1325 ν(COO_{sym}); 231 (Δν); 560 ν(Sn–C); 480 ν(Sn–O): **^{1}H NMR** (DMSO-d6, 300 MHz) δ (ppm): 2.61 (m, 4H, H2); 2.55 (m, 4H, H3); 12.17 (bs, 2H, NH); 7.43 (d, 2H, H6, ^3J[^{1}H, ^{1}H] = 3.6 Hz); 7.14 (d, 2H, H7, ^3J[^{1}H, ^{1}H] = 3.6 Hz); 1.02 (s, 6H, Hα) [$^{119/117}$Sn-^{1}H] = 113, 109 Hz): **^{13}C NMR** (DMSO-d6, 75 MHz) δ (ppm): 174.1 (C1); 30.2 (C2); 28.8 (C3); 170.6 (C4); 158.4 (C5); 138.0 (C6); 113.6 (C7); 23.0 (Cα, ^1J [$^{119/117}$Sn-^{13}Cα] = 957, 921 Hz).

2.2.7 Dibutylstannicbis[4-oxo-(thiazol-2-ylamino)]butanoate (4)

Yield: 80 %: M.p. 146-148 °C: elemental anaysis: % (calculated) for $C_{22}H_{32}N_4O_6S_2Sn$: C, 41.85 (41.81); H, 5.11 (5.13); N, 8.87 (8.83); S, 10.16 (10.12): **IR** (4000–250 cm^{-1}): 3358 ν(NH); 1699 ν (amide C=O); 1548 ν(COO_{asym}); 1329 ν(COO_{sym}); 219 (Δν); 552 ν(Sn–C); 443 ν(Sn–O): **^{1}H NMR** (DMSO-d6, 300 MHz) δ (ppm): 2.64 (m, 4H, H2); 2.56 (m, 4H, H3); 12.14 (bs, 2H, NH); 7.43 (d, 2H, H6, ^3J[^{1}H, ^{1}H] = 3.6 Hz); 7.16 (d, 2H, H7, ^3J[^{1}H, ^{1}H] = 3.6 Hz); 1.63 (m, 4H, Hα); 1.50 (m, 4H, Hβ); 1.28 (m, 4H, Hγ); 0.86 (t, 6H, Hδ, ^3J[^{1}H, ^{1}H] = 7.2 Hz): **^{13}C NMR** (DMSO-d6, 75 MHz) δ (ppm): 174.2 (C1); 32.8 (C2); 30.2 (C3); 170.6 (C4); 158.2 (C5); 138.0 (C6); 113.6 (C7); 38.1 (Cα, ^1J[$^{119/117}$Sn-^{13}Cα] = 867, 816 Hz); 28.1 (Cβ, ^2J [$^{119/117}$Sn-^{13}Cβ] = 46, 44 Hz); 26.0 (Cγ, ^3J[$^{119/117}$Sn-^{13}Cγ] = 157, 149 Hz); 14.2 (Cδ).

2.2.8 Diphenylstannicbis[4-oxo-(thiazol-2-ylamino)]butanoate (5)

Yield: 74 %: M.p. 99–100 °C: Mol. Wt.: 672.02: elemental anaysis: % (calculated) for $C_{26}H_{24}N_4O_6S_2Sn$: C, 46.52 (46.49); H, 3.60 (3.58); N, 8.35 (8.31); S, 9.55 (9.52): **IR** (4000–250 cm^{-1}): 3341 ν(NH); 1698 ν (amide C=O); 1554 ν(COO_{asym}); 1332 ν(COO_{sym}); 222 (Δν); 267 ν (Sn–C); 449 ν(Sn–O): **^{1}H NMR** (DMSO-d6, 300 MHz) δ (ppm): 2.71 (m, 4H, H2); 2.64 (m, 4H, H3); 12.16 (bs, 2H, NH); 7.44 (d, 2H, H6, ^3J[^{1}H, ^{1}H] = 3.6 Hz); 7.18 (d, 2H, H7, ^3J[^{1}H, ^{1}H] = 3.6 Hz); 7.91 (m, 4H, Hβ); 7.37 (m, 4H, Hγ); 7.28 (m, 2H, Hδ): **^{13}C NMR** (DMSO-d6, 75 MHz) δ (ppm): 173.0 (C1); 30.1 (C2); 28.5 (C3); 170.4 (C4); 158.3 (C5); 138.0 (C6); 113.7 (C7); 138.7 (Cα, ^1J[$^{119/117}$Sn-^{13}Cα] = 670, 630 Hz); 127.2 (Cβ, ^2J[^{119}Sn-^{13}Cβ] = 90 Hz); 135.1 (Cγ, ^3J[^{119}Sn-^{13}Cγ] = 70 Hz); 128.4 (Cδ).

2.3 Semi-empirical Study

Semi-empirical studies of the synthesized complexes were carried out by using MOPAC 2007 [11] program in the gas phase using PM3 method [12]. Selected parts of the complexes without metal ion were pre optimized using molecular mechanics method. Several cycles of energy minimization were made for all the complexes. The optimized geometry of the complexes was validated by using Eigen Vectors. The determined Root Mean Square Gradient for all the investigated molecules was less than one. Self-Consistent Field was achieved in each case. The absences of imaginary frequencies were exanmined consistently.

2.4 DNA Interaction Study Assay by UV–Visible Spectroscopy

0.3 g of SS-DNA (salmon sperm-DNA) was dissolved in 100 mL of distilled water and stirred for 2 days at 4 °C. Buffer solution of pH 7.3 was prepared by mixing appropriate volumes of 20 mM solutions of NaH_2PO_4 and Na_2HPO_4. A solution of SS-DNA in this buffer solution gave a ratio of UV absorbance at 260 and 280 nm (A_{260}/A_{280}) of 1.8, showing that the DNA is sufficiently free of protein [13]. The DNA concentration was determined by the absorption measurement at 260 nm using the molar absorption coefficient of 6600 M^{-1} cm^{-1} [14, 15] and was found to be 1.76×10^{-4} M. Working solutions were prepared by the appropriate dilution of this stock solution. The complexes were dissolved in 10 % DMSO at a concentration of 3×10^{-5} M. The UV absorption titrations were performed by keeping the concentration of complexes constant while varying the concentration of DNA. Equivalent solutions of DNA were added to the complex and reference solutions to eliminate the absorbance of DNA itself. Complex DNA solutions were incubated for 30 min. at ambient temperature before absorption measurements. The absorption measurements were recorded using cuvettes of 1 cm path length.

2.5 Antibacterial Assay

The synthesized complexes were screened for their antibacterial activity against five bacterial strains: *Staphylococcus aureus* (ATCC 6538), *Bacillus subtilis* (ATCC 6633), *Micrococcus luteus* (ATCC 53598), *Escherichia coli* (ATCC15224) and *Bordetella bronchiseptica* (ATCC 4617) by using disc diffusion method [15]. Stock solution of each complex, was prepared by dissolving 10 mg of complex in 1 mL of DMSO. 30 μg/disc concentration of each complex was used in the assay. Bacterial inoculum were prepared in nutrient broth by dissolving 2 g nutrient

broth in 100 mL of water (pH 7). Respective bacterial strains were streaked on labelled solidified plates of nutrient agar and 10 μL of each complex solution was absorbed on disc. These discs in respective petri plates were incubated for 24 h at 28 °C. Cefixime and roxythromycin were used as standard drugs and their stock solutions were prepared in DMSO. DMSO was used as negative control. Zones of inhibition were measured after 24 h.

2.6 Antifungal Assay

The antifungal assay of synthesized compounds was determined by using the disc diffusion method [15] against five fungal strains i.e., *Fusarium solani* (FCBP 0291), *Aspergillus nigar* (FCBP 0198), *Aspergillus flavis* (FCBP 0064), *Mucor species* (FCBP 0300) and *Helminthosporium solani* (FCBP 252). Sabouraud dextrose agar (SDA) (Sigma-Aldrich Germany) medium was autoclaved at 121 °C for 15 min. 25 mL medium was poured into pre-sterilized petri plates and allowed it to solidify at room temperature. Each fungal culture was streaked on petri plates. 5 μL sample solutions (20 mM prepared in DMSO) were poured on sterilized filter paper disc at final concentration of 100 μM. Placed these discs on media and incubated plates at 37 °C for 24 h. Turbinafine (1 mg mL^{-1}) and DMSO were used as positive and negative control, respectively. The diameter of these zones around each disc was measured. Triplicate plates were prepared for each fungal strain and average of these three plates was carried out.

2.7 Brine Shrimp Lethality Assay

The cytotoxicity of the complexes was studied by Brine shrimp lethality bioassay [16, 17]. Samples stock solutions (40,000 ppm) were prepared by dissolving 10 mg of complex in DMSO separately. Diluted solutions of (100, 50 and 10 ppm) were prepared by appropriate dilutions of the stock solutions. Brine shrimp (Artemia salina) eggs (Sera, Heidelberg, Germany) were hatched in artificial sea water present in shallow rectangular dish (22 × 32 cm). Sea water was prepared with a commercial salt mixture in distilled water. A plastic divider with several holes of 2 mm size was clamped in the dish to make two unequal compartments i.e. one was large and the other was small. Brine shrimp eggs (25 mg) were sprinkled in the large, dark compartment, (covered with aluminium foil), while the smaller compartment was illuminated. As hatching started, after 24 h phototropic nauplii (brine shrimp larvae) were collected by pipette from the lightened side.

Bioassay Two-dram vials were used for this bioassay. To prepare final concentration of 100, 50 and 10 ppm, each solution was taken in separate vials. For control, 0.5 mL of methanol and 0.5 mL of chloroform was taken. The solvent was allowed to evaporate over night and then put it in high vacuum for 3 h to ensure complete evaporation of the solvent. Three replicates were prepared for each concentration. Ten shrimps were transferred to each vial using Pasteur pipette, and artificial sea water was added to make up the volume up to 5 mL. The nauplii can be counted macroscopically in the stem of pipette against a light background. The vials were maintained under illumination at room temperature 25–28 °C. Survivors were counted with the aid of ×3 magnifying glass after 24 h. In case, where control death occurred, the data were corrected using Abbott's formula [18].

$$\% \, Death = \left[\frac{(\text{Test} - \text{Control})}{\text{Survivors of the control}} \right] \times 100$$

The LD$_{50}$ value was calculated by using Finny software [19].

2.8 Antileishmanial Assay

Leishamaniatropica kwh23 strain was maintained in fresh medium 199 (Merck KGaA, Germany) at 24 °C for 7 days to get the log phase of growth. The medium contained Fetal Bovine Serum at a concentration of 10 %. The experiment was performed as per procedure of Nabi et al., with slight modification [20]. Stock solutions of 10,000 ppm of the compounds were prepared in DMSO. The assay was carried out at different concentrations (200–0.02 ppm). The medium containing cultures were inoculated in 96 well plates and incubated with test samples at 24 °C for 24 h after serial dilution. Positive (Amphotericin B) and negative (DMSO) control of the assay was also maintained. All experiments were conducted in triplicate. After the required time of incubation, the live parasites of Leishmania were counted using neobar chamber under compound microscope. The data was statistically analyzed through Graph Pad Prism software 5.0.

2.9 Protein Kinase Inhibition Study

Protein kinase inhibition study of the synthesized complexes was performed by disc diffusion method [15]. Streptomyces (Actinobacter) culture was used for determination of protein kinase inhibition. Tryptic soya broth (Merck) was autoclaved at 121 °C for 15 min. and the strain was refreshed in the sterilized media for 24 h at 30 °C. Mineral media were prepared using various salts and were autoclaved under similar conditions as those of Tryptic soya broth. Media was poured into pre-sterilized petri plates and allowed to solidify at room temperature. After setting activated streptomyces strain was swabbed on

solidified media with the help of sterilized cotton plug. The test samples were prepared in DMSO (20 mM) and 5 μL of the solution was placed on a sterilized filter paper disc at the final concentration of 100 μM. The discs were placed above media in their respective labeled positions and were incubated at 28 °C for 48–72 h. After an incubation period balled zones around each disc with no growth were measured to determine the protein kinase inhibition activity of the samples. The assay was performed in triplicate and average reading was taken.

3 Results and Discussion

3.1 FT-IR Spectra

The identification of the binding mode of the COO⁻ moiety with tin atom was made by the comparison of the FTIR spectra of the synthesized ligand and its complexes. The appearance of a new Sn–O band in the region of 443–480 cm⁻¹ indicated the coordination with di- and triorganotin(IV) moieties via oxygen atoms of the COO⁻ group [21–23] after deprotonation of the ligand. The band in the range of 552–574 cm⁻¹ indicated the presence of Sn–C bonds for complexes **1**, **3** and **4** while the same bands appeared at 267 and 277 cm⁻¹ for di- and triphenyltin complexes **2** and **5** respectively. The difference between $\nu_{asym}(COO)^-$ and $\nu_{sym}(COO)^-$ ($\Delta\nu$) is important to find out the binding mode of COO⁻ moiety with Sn atom. The $\Delta\nu$ value greater than 250 cm⁻¹ indicates a monodentate while a value less than 250 cm⁻¹ shows a bidentate binding mode of COO⁻ moiety with tin atom [22]. Moreover a $\Delta\nu$ value in the range of 150–250 cm⁻¹ indicates a bridging behaviour while a value <150 cm⁻¹ exhibits a chelate structure [24]. In the present study, the $\Delta\nu$ values for complexes **2–5** were found to be 154, 219, 231 and 222 cm⁻¹, respectively, compared to its sodium salt 246 cm⁻¹, revealing bidentate binding mode of COO⁻ moiety with tin atom. While the observed $\Delta\nu$ value of 249 cm⁻¹ for complex **1** showed monodentate nature of the carboxylate group, probably due to steric effect of n-butyl groups. The results of FT-IR study are consistent with the X-ray crystallographic data.

3.2 NMR Spectral Studies

The ¹H NMR spectra of the synthesized ligand **HL** and its complexes **1–5** were interpreted by the multiplicities and integration patterns of their protons. The characteristic peak for the OH bond in the spectrum of the ligand at 12.17 ppm is not present in spectra of the complexes, indicating the deprotonation of the ligand during complexation with organotin(IV) species which is consistent with the IR data.

There was no significant change in the position of the NH signal of the peptide linkage in the spectra of the complexes indicating that nitrogen is not involved in coordination with tin. According to the literature, the coordination pattern of tin(IV) in di- and triorganotin(IV) derivatives with the $^{1}J[^{119}Sn-^{13}C]$ and $^{2}J[^{119}Sn-^{1}H]$ coupling constant values are as: in tetra coordinated tin compounds ^{1}J values are predicted to be smaller than 400 Hz whereas ^{2}J values should be below 59 Hz; for penta coordinated tin, ^{1}J values fall in the range of 450–550 Hz and the ^{2}J values in the range of 65–80 Hz; finally, for hexa coordinated tin ^{1}J and ^{2}J values are generally larger than 600 and 83 Hz, respectively. The determined values (113/109) of $^{2}J[^{119/117}Sn, ^{1}H]$ coupling constant for complex **3** indicated hexa coordinated behavior of tin(IV) atom in solution [9]. In complexes, **1** and **4** the terminal methyl protons of butyl groups attached to the tin atom showed a clear triplet at 0.83–0.86 ppm, while the rest of the protons showed a complex multiplicity pattern. The protons of phenyl moiety generally show a complex pattern in the range of 7.26–7.89 ppm and were assigned according to the literature [25–27].

The ¹³C NMR data, values of coupling constants $^{1}J [^{119}Sn, ^{13}C]$ and C–Sn–C angles are helpful to find out the coordination behavior of tin(IV) atom in solution and were calculated by Lockhart's equation [28] and the values are reported in Table 1. The complexes **2–5** exhibited $^{1}J [^{119}Sn, ^{13}C]$, 639 Hz (116°), 957 Hz (170°), 867 Hz (161°) and 670 Hz (118°), respectively, which correspond to penta/hexa coordinated tin(IV) atom in solution. The results are consistent with literature [29, 30]. The tendency of complexes **3–5** ranging from five coordination to six may be due to their fluxional behavior [31]. The observed coupling constant $^{1}J [^{119}Sn, ^{13}C]$, 474 Hz (122.0) for complex **1** corresponds to four coordinated tin(IV) atom in solution which is in accordance with the literature value [32]. The calculated C–Sn–C angle (122.0) in complex **1** by Lockhart's equation also supports a four coordinated geometry of tin(IV) atom in solution.

Table 1 (C–Sn–C) angles (°) based on NMR parameters of **1–5** complexes

Complex no.	$^{1}J[^{119}Sn, ^{13}C]$ (Hz)	$^{2}J[^{119}Sn, ^{1}H]$ (Hz)	Angles (°)	
			^{1}J	^{2}J
(**1**)	474	–	122	–
(**2**)	639	–	116	–
(**3**)	957	113	170	166
(**4**)	867	–	161	–
(**5**)	670	–	118	–

Table 2 Crystal and structure refinement data of complex (**1**)

Identification code	(**1**)
Empirical formula	$C_{19}H_{34}N_2O_3SSn$
Formula weight	490.13
Temperature (K)	296(2)
Crystal system	Monoclinic
Space group	P 2_1/n
a (Å)	10.5389(6)
b (Å)	13.7989(9)
c (Å)	16.6702(12)
α (°)	90
β (°)	100.323(2)
γ (°)	90
Volume (Å^3)	2385.0(3)
Z	4
ρ_{calc} (mg mm^{-3})	1.357
m mm	1.177
F(000)	1000.0
Crystal size (mm^3)	0.30 × 0.20 × 0.17
Radiation	MoKα (λ = 0.71073)
2Θ range for data collection	3.858°–54.276°
Index ranges	$-13 \leq h \leq 13, -17 \leq k \leq 14, -20 \leq l \leq 21$
Reflections collected	19,866
Independent reflections	5261 [R_{int} = 0.0275, R_{sigma} = 0.0321]
Data/restraints/parameters	5261/18/212
Goodness-of-fit on F^2	1.004
Final R indexes [I $\geq 2\sigma$ (I)]	R_1 = 0.0506, wR_2 = 0.1419
Final R indexes (all data)	R_1 = 0.1071, wR_2 = 0.1818
Largest diff. peak/hole (e Å^{-3})	0.54/−0.47

Table 3 Selected bond lengths (Å) and bond angles (°) of complex 1

Selected bond lengths (Å)			
C1–C2	1.472(9)	C8A—Sn1	2.128(14)
C1–O1	1.301(7)	C8B—Sn1	2.10(2)
C1–O2	1.196(7)	C12A—Sn1	2.125(13)
O1–Sn1	2.109(4)	O2—Sn1	3.004(5)
Selected bond angles (°)			
O1–C1–C2	114.2(6)	O2—C1—C2	121.0(6)
O3–C4–N1	122.6(6)	N1—C5—S4	124.7(4)
C9A–C8A–Sn1	103.7(10)	C12A—Sn1—C16A	121.2(5)
C13A–C12A–Sn1	117.3(13)	C1—O1—Sn1	114.4(4)
C16A–Sn1–C8A	122.6(5)	O1—Sn1—C12A	102.0(4)
O1–Sn1–C8A	94.1(5)	O1—Sn1—C12B	98.0(5)

3.3 X-ray Crystallography

3.3.1 Crystal Structure of Complex 1

The crystal data, structure refinement parameters, selected bond lengths and angles of complex **1** are given in Tables 2
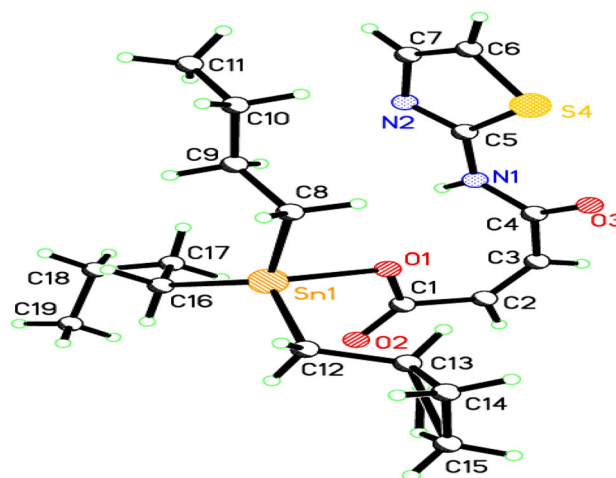
Fig. 1 ORTEP drawing of the complex Bu$_3$SnL (**1**) showing the crystallographic numbering scheme

and 3, while its ORTEP drawing exhibiting the crystallographic numbering scheme is shown in Fig. 1. The geometry around the tin atom is distorted tetrahedral

defined by three butyl groups and one oxygen atom. The C–Sn–C and O–Sn–C angles [C–Sn–C = 102.5°–122.6° and O–Sn–C = 94.2°–96.6°] are within the expected range of four-coordinated tetrahedral geometry and in close agreement with the reported values of similar complex [33]. The distance of Sn1–O2 (3.004 Å) is longer than the normal Sn–O1 (2.109 Å) bond length, therefore, O2 do not participate in coordination with the tin atom (Fig. 1). The sum of the C-Sn-C angles equals 346.2°, indicating slight distortion in a tetrahedral geometry as reported in the literature [5]. There are intramolecular N–H–O (O of the amide carbonyl group)and S–O (O of the amide carbonyl group) interactions within the polymeric chain. The intermolecular N–H–O and S–O interaction links the polymeric chains in sheets form or zigzag form which are linked into a three-dimensional network. It is interesting to note that in solid state, the complex "1" exists in polymeric form, but in solution form, it behaves as a normal coordinated complex.

3.4 Semi-empirical Study

In geometrically optimized structures of complexes **3** and **5**, the ligand act as a bidentate through both oxygen atoms of the carboxylate group which was confirmed by FT-IR and NMR data. The other positions are occupied by methyl or phenyl groups. The computed bond angles and bond lengths of the ligand **HL,** complexes **3** and **5** are listed in Table 4, while the thermodynamic parameters and molecular descriptors have been reported in Tables 5 and 6, respectively. The bond lengths Sn–C and Sn–O are in accordance with the reported values for the similar compounds [34]. Computed negative heat of formation indicates that **3** and **5** are thermodynamically stable (Table 5). The complex **3** is more stable as compared to **5**, since the farmer has a lower heat of formation, enthalpy, entropy and heat capacity. The calculated HOMO and LUMO orbitals of **HL, 3,** and **5** are shown in Figs. 2, 3 and 4. In case of **HL,** HOMO and LUMO orbitals lie on the heterocyclic ring and CO–NH moiety. In case of **3** and **5,** LUMO lies

primarily on the tin and the atoms ligating to tin, while the HOMO orbitals lie on the hetrocylcic ring and the CO–NH atoms. A large HOMO–LUMO gap indicates stable molecule, while a small E_{HOMO} is associated with an unstable molecule with high chemical reactivity. The ability of the molecule to donate electrons, (-ionization potential), E_{LUMO} represents (-electron affinity), and electrophilicity values ($\omega = \mu2/2\eta$) [35], chemical potential values $\mu = - (I + A)/2$ [36], global hardness ($\eta = I - A/2$) values [37] and global softness values ($S = 1/2\eta$) [38], have been calculated for **HL, 3** and **5,** and the results were shown in Table 6, which revealed that as the HOMO–LUMO gap decreases, the global hardness and chemical potential decreases, while global softness and electrophilicity increases. Complex **3** has a larger HOMO–LUMO gap than **5**, therefore, is harder and stable.

3.5 DNA Binding Study by UV–Vis Spectroscopy

The interaction of complexes with DNA was examined by UV–Vis spectroscopy, in order to get some information about their mode of interaction and binding strength. The comparison of absorbance and a shift in the wavelength of ligand and complexes with and without SS-DNA, give the idea about the interaction of ligand or metal complexes with DNA [39]. Figures 5, 6 and 7 show the representative UV–vis spectra when compounds (**HL**, **2** and **5**) interact with different concentrations of DNA.The magnitude of this shifting could be interpreted as an indication of the strength of the interaction between the DNA structure and the compound under consideration [40–43]. There is one band in the range of 268-311 nm for complexes **1–5**, due to the transition between n − π* energy level of the coordinated compound. With increasing DNA concentration, the absorption bands exhibit hypochromism along with bathochromic as well as in some cases hypsochromic shift. The peculiar hypochromism observed is attributed to the intercalation of these complexes into the DNA base pairs [44, 45]. Hypochromism along with bathochromic shift is consistent with the combination of π electrons of the

Table 4 Selected bond angles (°) and bond lengths (Å) of **HL,** complex **3** and **5**

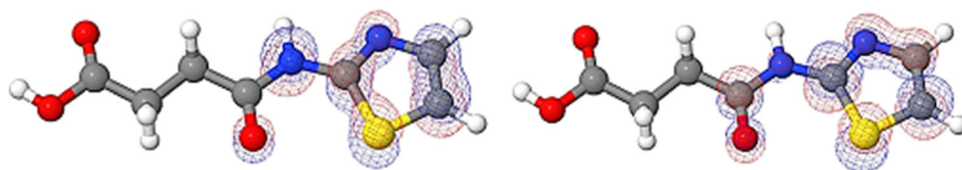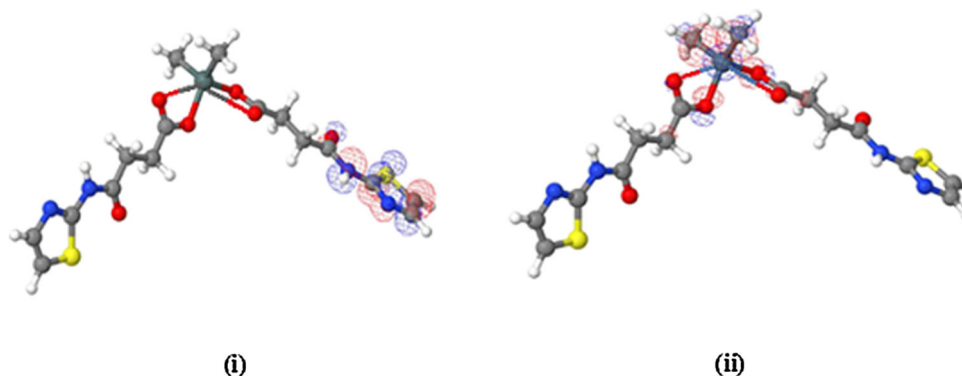|	HL	(3)	(5)
Bond angles (°)			
C–Sn–C	–	114.9	113.7
O–Sn–O	–	97.4	110.7, 110.3
C–Sn–O	–	98.5, 108.4, 112.7, 121.2	99.9, 107.7, 122.5, 112.0
Bond lengths (Å)			
C–Sn	–	2.08, 2.08	2.05, 2.5
O–Sn	–	2.01, 2.02	2.00, 2.01
C–O	1.35, 1.22	1.32, 1.24, 1.24, 1.32	1.32, 1.24, 1.24, 1.32
C–S	1.73, 1.77, 1.73, 1.77	1.73, 1.77, 1.73, 1.77	1.73, 1.77, 1.73, 1.77

Table 5 Computed thermodynamic parameters of **HL** and complexes **3** and **5**

Parameters at 298 K	**HL**	**(3)**	**(5)**
Heat of formation (kcal mol^{-1})	−92.662	−190.733	−118.888
Enthalpy (kcal mol^{-1})	6783.50	14212.02	16320.76
Entropy (kcal mol^{-1} K^{-1})	99.03	152.33	164.33
Heat capacity(Cp) (cal mol^{-1} K^{-1})	40.91	91.84	111.00

Table 6 Computed molecular descriptors of **HL** and complexes **3** and **5**

Descriptors	**HL**	**(3)**	**(5)**
E$_{HOMO}$ (eV)	−9.18	−9.126	−9.140
E$_{LUMO}$ (eV)	−0.701	−0.908	−1.040
HOMO–LUMO (eV)	8.486	8.218	8.099
Global hardness (η, eV)	4.243	4.108	4.049
Global softness (S, eV^{-1})	0.117	0.121	0.123
Chemical potential (μ, eV)	−4.938	−5.016	−5.089
Electrophilicity (ω)	2.874	3.062	3.198
Dipole moment (debyes)	0.041	1.512	1.361

compound with π electrons of DNA bases. Consequently, the energy level of the π–π* electron transition decreases, which causes a red shift [46] while the hypochromism along with hypsochromic shift may be attributed to the strong hydrogen bonding of the interacting chromophore with the base pairs of the DNA due to the presence of an electronegative nitrogen atom on the coordinated ligand. The non-bonding lone pair on nitrogen atom involved in hydrogen bonding with DNA base pairs resulting in stabilization of non-bonding orbital, thus increasing the n − π* transition energy which results in blue shift. Based upon the variation in absorbance, the intrinsic binding

constant of these complexes with DNA were determined according to Benesi–Hildebrand equation [47].

$$\frac{A_0}{A - A_0} = \frac{\varepsilon_G}{\varepsilon_{H-G}-\varepsilon_G} + \frac{\varepsilon_G}{\varepsilon_{H-G}-\varepsilon_G}\frac{1}{K[DNA]}$$

where K is the binding constant, A$_0$ is the absorbances of the drug, A is the absorbances of the complex with DNA adduct, ε_G is the absorption coefficients of the drug and ε_{H-G} is the absorption coefficients of the drug and drug-DNA complex.

The binding constants were obtained from the intercept to slope ratios of A$_0$/(A − A$_0$) versus 1/[DNA] plots and are shown in Table 7. The Gibbs's free energy (ΔG) value was determined from the equation:

$$\Delta G = -RT \ln K$$

where R is the general gas constant (8.314 JK^{-1} mol^{-1}) and T is the temperature (298 K). The interaction of these drugs is a spontaneous process as attested by negative values of ΔG (Table 7). The binding constant values show that triorganotin(IV) derivatives have higher binding constant than their diorganotin(IV) analogues probably due to more lipophilic character. Stronger interaction will lead to more alteration in the replication machanism of DNA and thus cancerous cell division will be prevented.

Fig. 2 HOMO (**i**) and LUMO (**ii**) orbitals of **HL**
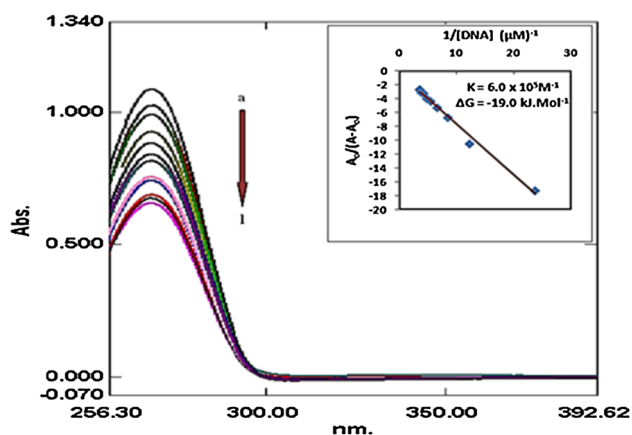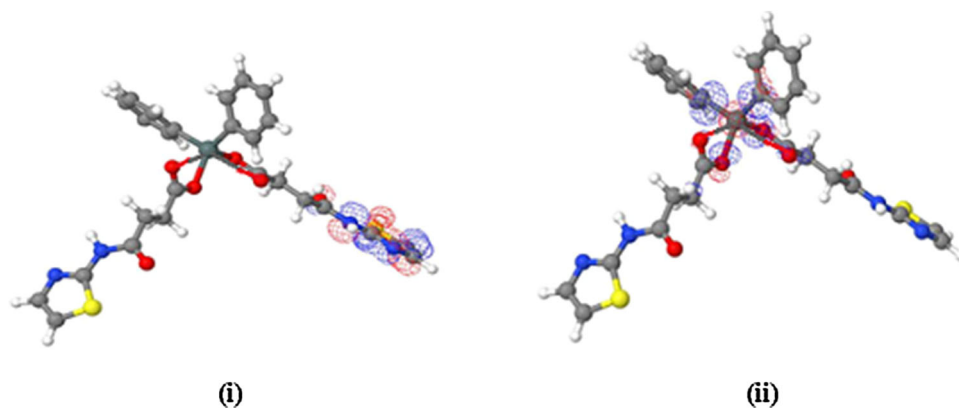

Fig. 3 HOMO (**i**) and LUMO (**ii**) orbitals of Me$_2$SnL$_2$ (**3**)

(i) (ii)

Fig. 4 HOMO (**i**) and LUMO (**ii**) orbitals of Ph_2SnL_2 (**5**)

(i)

(ii)

Fig. 5 Absorption spectrua of 2 mM of (**HL**) in the absence (*a*) and presence of 9 (*b*), 18 (*c*), 27 (*d*), 36 (*e*), 45 (*f*), 54 (*g*), 63 (*h*), 72 (*i*), 81 (*j*), 90 (*k*), and 99 (*l*) μM DNA. The *arrow direction* indicates increasing concentrations of DNA

Fig. 7 Absorption spectra of 2 mM of (**5**) in the absence (*a*) and presence of 9 (*b*), 18 (*c*), 27 (*d*), 36 (*e*), 45 (*f*), 54 (*g*), 63 (*h*), 72 (*i*), 81 (*j*) and 90 (*k*) μM DNA. The *arrow direction* indicates increasing concentrations of DNA
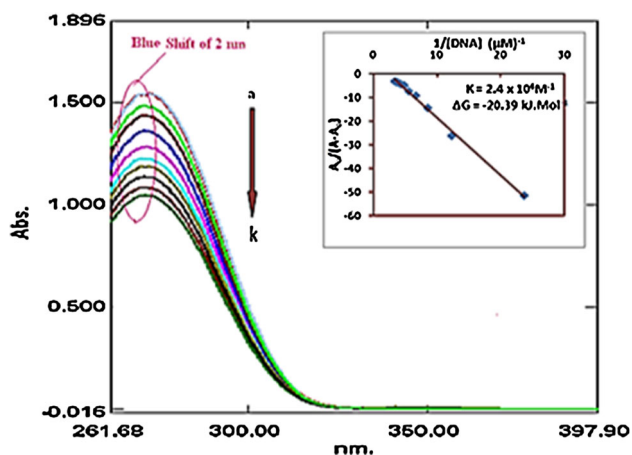
Fig. 6 Absorption spectra of 2 mM of (**2**) in the absence (*a*) and presence of 9 (*b*), 18 (*c*), 27 (*d*), 36 (*e*), 45 (*f*), 54 (*g*), 63 (*h*), 72 (*i*), 81 (*j*) and 90 (*k*) μM DNA. The *arrow direction* indicates increasing concentrations of DNA
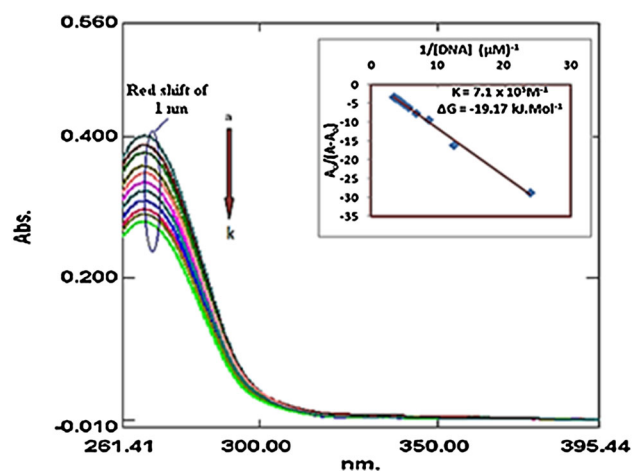
Table 7 Determined binding constants and Gibb's free energies for ligand **HL** and its complexes **1–5**

Complex no.	K (M^{-1})	$-\Delta G$ (kJ mol^{-1})
HL	6.0×10^5	19.0
1	1.8×10^6	20.1
2	2.4×10^4	20.3
3	1.8×10^6	20.1
4	1.6×10^6	19.9
5	7.1×10^5	19.1

3.6 Biological Activities

3.6.1 Antibacterial Activity

In vitro biological screening tests of the synthesized ligand **HL** and its organotin(IV) complexes were carried out

against three gram-positive [*Bacillus subtillis* (ATCC 6633), food poisoning; *Staphylococcus aureus* (ATCC 6538), food poisoning, scaled skin syndrome, endrocarditis, *Micrococcus luteus* (ATCC 53598), recurrent bacteremia, septic shock, septic arthritis, endocarditis, meningitis, and cavitating pneumonia] and two gram-negative bacteria [*Escherichia coli*, (ATCC 15224), infection of wounds, urinary tract and dysentery; *Bordetella bronchiseptica* (ATCC 4617), atrophic rhinitis]. The assay was performed in triplicate by disc diffusion method [15]. Cefixime was used as positive control. The results are shown in Table 8. Criteria for activity is based on the inhibition zone size (mm) i.e., >20 mm shows significant activity, 18–20 mm is good, 15–17 mm is low, and below 11–14 mm is non-significant [13]. The antibacterial results showed that all compounds except ligand **HL** have activity toward tested pathogen strains. Complexes **1**, **2** and **4**, exhibited significant activity against pathogenic strains, *B. subtillis*, *M. luteus* and *S. aureus* while complex **3** has low to non-significant activity against all the tested pathogenic strains and complex **5** showed good activity against *E. coli.* This shows that the activity of the ligand increases upon complexation which reduces the polar nature of the tin atom by the delocalization of electrons and sharing of charge with the donor group [48, 49]. Thus, the lipophilic nature of tin atom increases, which enhances the permeability of compounds through the plasma membrane. As a result, they can reach the site of action within the cell easily where tin may either involve in ligand exchange by the donor atoms present in enzymes, DNA and protein or polar group of the ligand develop H-bonds/non-covalent interactions with the active center of cellular constituents. These structural changes may ultimately end up with death of the microorganism [50, 51].

3.6.2 Antifungal Activity

The antifungal activity of the ligand **HL** and its organotin(IV) complexes **1–5** was tested against five fungal strains (*Aspergillus nigar*, *Fusarium solani*, *Mucor species*, *Helminthosporium solani*, and *Aspergillus flavus*) by using disc diffusion method in vitro [15]. The results are shown in Table 9. Terbinafine was used as standard drug in this assay. The criteria for activity is based on percent growth inhibition i.e., 70, 60–70, 50–60 and below 50 %, are considered as significant, good, moderate and non-significant, respectively [46]. The results showed that complexes **1** and **2** exhibited 100 % growth inhibition against all the tested strains while complexes **4** and **5** showed moderate to significant activity except for *F. solani*. However, complex **3** exhibited 100 % growth inhibition against *A. flavus* only and non-significant for rest of the tested strains. The results of the present study are consistent with literature that triorganotin compounds are more biocidally active as compared to diorganotin compounds probably due to the increased lipophilicity and easy permeation through the lipid layer of cell membrane [52, 53].

3.6.3 Cytoxicity

The cytotoxicity was studied by the brine shrimp lethality method and the results are summarized in Table 10. Compared to standard drug, highest toxicity was shown by complexes **1**, **2**, **4** and **5** with LD_{50} value <10 µg mL^{-1}, while lowest toxicity was observed for **HL** and complex **3** with LD_{50} values in the range of 121.3 and 50.4 µg mL^{-1}, respectively. This can be explained in terms of ligand's toxicity and the degree of hydrophilicity of the complexes [3]. In addition, diorganotin(IV) compounds can affect the cellular metabolism, while triorganotin(IV) compounds mediate an exchange of hydroxyl ions across the mitochondrial membranes [54, 55].

3.6.4 Antileishminial Activity

The antiprotozoal activity of the **HL** and its organotin(IV) complexes **1–5** against pathogenic Leishmania was studied and results are summarized in Table 11. The synthesized

Table 8 Antibacterial data of (**HL**) and its organotin(IV) complexes

Complex no.	B. subtillis	M. luteus	S. aureus	E. coli	B. bronchiseptica
			Zone of inhibition (mm)		
HL	–	15	–	–	–
1	22	20	25	11	14
2	24	29	19	10	21
3	–	9	11	5	–
4	22	23	16	16	16
5	18	19	–	22	16
Cefixime	29	32	35	37	30

In vitro, disc diffusion method, conc. 1 mg mL^{-1} of DMSO, inhibition zone in mm

Reference drug, Cefixime

Table 9 Antifungal data of (**HL**) and its organotin(IV) complexes

Complex no.	% Growth inhibition				
	Fusariumsolani	*Aspergillusnigar*	*Mucor species*	*Helminthosporiumsolani*	*Aspergillusflavus*
HL	20	5	15	0	40
1	100	100	100	100	100
2	100	90	100	100	100
3	20	30	35	15	100
4	15	55	70	20	80
5	0	75	80	90	100
Turbinafine	100	100	100	100	100
DMSO	0	0	0	0	0

In vitro, disc diffusion method, conc. 1 mg mL^{-1} of DMSO, Growth inhibition in %

Reference drug, Turbinafine

Table 10 Cytotoxicity data of ligand (**HL**) and its organotin(IV) complexes against brine shrimps in vitro

No of shrimps killed out of 20 per dilution

Complex no.	100 µg mL^{-1}	50 µg mL^{-1}	10 µg mL^{-1}	LD$_{50}$
HL	8	5	2	121.3
(**1**)	20	20	20	<10
(**2**)	20	20	20	<10
(**3**)	20	9	3	50.38
(**4**)	20	20	18	7.44
(**5**)	20	18	15	3.15

Compared with standard drug MS-222 (tricainemethanesulfonate) with LD$_{50}$ value of 4.30 µg mL^{-1}

Table 11 Antileishminial data of the ligand (**HL**) and its organotin(IV) complexes

Complex no.	LC$_{50}$ (µg mL^{-1})
HL	1.532
1	0.0012
2	0.007
3	4.001
4	0.173
5	0.961
Amphotericin B	0.048

Incubation temperature: 22 °C

compounds showed a significant reduction in viable promastigotes. The minimum protozoa concentration (IC$_{50}$) for promastigotes, defined as the concentration that results in 50 % reduction in parasites after 72 h incubation [56]. Among the synthesized compounds **1** and **2** exhibited strong antileishmanial activity that was even higher than that of control amphotericin B with significant cytotoxicity. It may be due the interference in the function of parasitic mitochondria thus disturbing the respiration process causing the death of microorganisms.

3.6.5 Protein Kinase Inhibition Study

Protien kinase is the preliminary assay of antitumor activity, illustrating a divergent class particularly for the inhibition of kinases. It blocks the aerial hyphae formation of *Streptomyces species,* induced by kinases, and thus may be hypothesized to inhibit the cancer cell proliferation. Therefore the scientific community showed keen interest in kinase inhibition study leading to the new technique for

chemo preventive measures [57]. The results of the protein kinase inhibition of complexes (**1**–**5**) are summarized in Table 12, which reveals varying degree of zone inhibition (5.0 ± 0.70 to 10.0 ± 0.71 mm). Compound **4** was found to be most effective as it produced the maximum zone of inhibition on culture plates and may be considered as a potential candidate to inhibit the tumor initiation.

Since the synthesized complexes demean like monomers in solution (Sect. 3.3.1), the biological activities could be exclusively related to the organotin(IV) complexes i.e., R$_3$SnL and R$_2$SnL$_2$.

3.7 Structure Activity Relationship

From the results of biological activity, it is concluded that there is a direct relationship between the biocidal activity and the coordination environment of the tin. The function of the ligand is to support the transport of the active organotin moiety to the site of action where it is released by hydrolysis. As

Table 12 Protein kinase inhibition data of **HL** and its organotin(IV) complexes

Complex no.	Zone of inhibition (mm)
HL	8 ± 1.41
1	05 ± 0.70
2	07 ± 0.73
3	7 ± 1.70
4	10 ± 0.75
5	6.7 ± 0.70
Tyrab[a]	18 ± 0.70

[a] Standard: Tyrab

triorganotin(IV) complexes mostly adopt trigonal bipyramidal geometry in solution which is (confirmed by NMR and IR with few exceptions of tetrahedral geometry) have more space for incoming groups such as bacteria, fungi etc., show significant activity as compared to diorganotin(IV) complexes which have less room for the incoming groups probably due to hexacoordinated environment in solution [58].

4 Conclusions

The ligand 4-oxo-4-(thiazol-2-ylamino)butanoic acid was successfully synthesized and characterized. The ligand was treated with different di- and triorganotin(IV) chlorides to form corresponding complexes. The ligand coordinates through oxygen to the tin atom during complexation. UV–Vis spectroscopic investigation showed that the synthesized complexes bind to DNA via intercalative mode of interaction resulting in hypochromism with minor red or blue shift. The negative values of Gibb's free energy change confirmed the spontaneity of these interactions. HOMO–LUMO calculations showed that complexes **3** and **5** are thermodynamically more stable than the ligand **HL**. Biological studies revealed that generally triorganotin(IV) complexes have higher activities than their corresponding diorganotin(IV) analogues.

5 Appendix A. Supplementary Material

Crystallographic data for the structure reported in this paper for complex 1 have been deposited with the Cambridge Crystallographic Data Centre, CCDC#997235. Copies of these information may be obtained free of charge from The Director, CCDC, 12, Union Road, Cambridge CB2 1EZ [Fax: +44 (1223)336 033], or e-mail deposit@ccdc.cam.ac.uk or http://www.ccdc.cam.ac.uk.

References

1. M.S. Ahmad, M. Hussain, M. Hanif, S. Ali, M. Qayyum, B. Mirza, Chem. Biol. Drug Design **71**, 568–576 (2008)
2. M. Sirajuddin, S. Ali, F.A. Shah, M. Ahmad, M.N. Tahir, J. Iran. Chem. Soc. **11**, 297–313 (2014)
3. M. Khan, M.K. Baloch, M. Ashfaq, J. Organomet. Chem. **689**, 3370–3378 (2004)
4. Q. Li, M.F.C. Guedes da Silva, A.J. Pombeiro, Chem A. Eur. J. **10**, 1456–1462 (2004)
5. M. Sirajuddin, S. Ali, V. McKee, M. Sohail, H. Pasha, Eur. J. Med. Chem. **84**, 343–363 (2014)
6. E.R. Tiekink, Appl. Organomet. Chem. **5**, 1–23 (1991)
7. M. Hussain, M. Zaman, M. Hanif, S. Ali, M. Danish, J. Serbian Chem. Soc. **73**, 179–187 (2008)
8. A.G. Davies, P.J. Smith, Adv. Inorg. Chem. Radiochem. **23**, 1–77 (1980)
9. M.M. Amini, A. Azadmeher, H.R. Khavasi, S. Ng, J. Organomet. Chem. **692**, 3922–3930 (2007)
10. W.L. Armarego, C.L.L. Chai, *Purification of laboratory chemicals* (Butterworth-Heinemann, Amsterdam, 2013)
11. S. Hussain, S. Ali, S. Shahzadi, S.K. Sharma, K. Qanungo, M. Shahid, Bioinorg. Chem. Appl. **2014**, 717421 (2014)
12. J. Stewart, J. Comp. Chem **12**, 320–328 (1991)
13. M. Sirajuddin, S. Ali, N.A. Shah, M.R. Khan, M.N. Tahir, Spectrochim. Acta Part A **94**, 134–142 (2012)
14. C. Sastri, D. Eswaramoorthy, L. Giribabu, B.G. Maiya, J. Inorg. Biochem. **94**, 138–145 (2003)
15. T.R. Fritsche, P.F. McDermott, T.R. Shryock, R.D. Walker, J. Clin. Microbiol. **45**, 2758–2759 (2007)
16. Atta-ur-Rahman, M.I. Choudhary, W.J. Thomsen, *Bioassay Techniques for Drug Development* (Harwood Academic Publishers, Amsterdam, 2001)
17. B. Meyer, N. Ferrigni, J. Putnam, L. Jacobsen, D.J. Nichols, Planta Medica **45**, 31–34 (1982)
18. W. Abbott, J. Econ. Entomol. **18**, 265–267 (1925)
19. D. Finney, *Probit Analysis* (University Printing House, Cambridge, 1947)
20. S. Nabi, N. Ahmed, M.J. Khan, Z. Bazai, M. Yasinzai, Y. Al-Kahraman, World Appl. Sci. J. **19**, 1495–1500 (2012)
21. Q. Xie, Z. Yang, L. Jiang, Main Group Met. Chem. **19**, 509–520 (1996)
22. G. Eng, X. Song, A. Zapata, A.C. de Dios, L. Casabianca, R.D. Pike, J. Organomet. Chem. **692**, 1398–1404 (2007)
23. H.D. Yin, Q.B. Wang, Q.J. Xing, Heteroat. Chem. **15**, 524–529 (2004)
24. G. Deacon, R. Phillips, Coord. Chem. Rev. **33**, 227–250 (1980)
25. M.H. Bhatti, S. Ali, H. Masood, M. Mazhar, S.I. Qureshi, Synth. React. Inorg. Matel-Org. Chem. **30**, 1715–1729 (2000)
26. S. Ali, F. Ahmad, M. Mazhar, A. Munir, M.T. Masood, Synth. React. Inorg. Matel-Org. Chem. **32**, 357–372 (2002)
27. K. Shahid, S. Ali, S. Shahzadi, A. Badshah, K.M. Khan, G.M. Maharvi, Synth. React. Inorg. Matel-Org. Chem. **33**, 1221–1235 (2003)
28. T.P. Lockhart, W.F. Manders, E.M. Holt, J. Am. Chem. Soc. **108**, 6611–6616 (1986)
29. M. Nadvornik, J. Holeček, K. Handlíř, A. Lyčka, J. Organomet. Chem. **275**, 43–51 (1984)
30. J. Holeček, M. Nadvornik, K. Handlíř, A. Lyčka, J. Organomet. Chem. **315**, 299–308 (1986)
31. J.J. Bonire, G.A. Ayoko, P.F. Olurinola, J.O. Ehinmidu, N.S. Jalil, A.A. Omachi, Met.-Based Drugs **5**, 233 (1998)
32. D. Axelson, S. Kandil, C. Holloway, Can. J. Chem. **52**, 2968–2973 (1974)

33. T.S.B. Baul, E.R.T. Tiekink, Acta Crystallogr. Sect. C **52**, 1428–1430 (1996)
34. S. Shahzadi, S. Ali, J. Iran. Chem. Soc. **5**, 16–28 (2008)
35. R.G. Parr, L.V. Szentpaly, S. Liu, J. Am. Chem. Soc. **121**, 1922–1924 (1999)
36. R.G. Parr, R.A. Donnelly, M. Levy, W.E. Palke, J. Chem. Phys. **68**, 3801–3807 (1978)
37. R.G. Parr, R.G. Pearson, J. Am. Chem. Soc. **105**, 7512–7516 (1983)
38. W. Yang, R.G. Parr, Proc. Natl. Acad. Sci. **82**, 6723–6726 (1985)
39. S. Tabassum, G.C. Sharma, F. Arjmand, A. Azam, Nanotechnology **21**, 195102 (2010)
40. H. Sun, J. Xiang, Y. Liu, L. Li, Q. Li, G. Xu, Y. Tang, Biochimie **93**, 1351–1356 (2011)
41. J. Jaumot, R. Gargallo, Curr. Pharm. Design **18**, 1900–1916 (2012)
42. C. Wei, J. Wang, M. Zhang, Biophys. Chem. **148**, 51–55 (2010)
43. K. Bhadra, G.S. Kumar, Biochim. Biophys. Acta **1810**, 485–496 (2011)
44. X. Yang, G.-L. Shen, R.-Q. Yu, Microchem. J. **62**, 394–404 (1999)
45. Z. Xu, G. Bai, C. Dong, Bioorg. Med. Chem. **13**, 5694–5699 (2005)
46. M. Sirajuddin, S. Ali, A. Haider, N.A. Shah, A. Shah, M.R. Khan, Polyhedron **40**, 19–31 (2012)
47. M. Ibrahim, I. Shehatta, A. Al-Nayeli, J. Pharm. Biomed. Anal. **28**, 217–225 (2002)
48. R. Ramesh, M. Sivagamasundari, Synth. React. Inorg. Matel-Org. Chem. **33**, 899–910 (2003)
49. S. Dehnen, in Tin Chemistry, Fundamentals, Frontiers and Applications, chap. 4, ed. by A.G. Davies, M. Gielen, K.H. Pannell, E.R.T. Tiekink (2008), pp. 413–496
50. N. Muhammad, S. Ali, I.S. Butler, A. Meetsma, Inorg. Chim. Acta **373**, 187–194 (2011)
51. K. Nagashri, J. Joseph, C.J. Dhanaraj, Appl. Organomet. Chem. **25**, 704–717 (2011)
52. F.R. Abreu, D.G. Lima, E.H. Hamú, C. Wolf, P.A. Suarez, J. Mol. Catal. A **209**, 29–33 (2004)
53. Y. Shi, B.-Y. Zhang, R.-F. Zhang, S.-L. Zhang, C.-L. Ma, J. Coord. Chem. **65**, 4125–4136 (2012)
54. N.J. Snoeij, P.M. Punt, A. Penninks, W. Seinen, Biochim. Biophys. Acta **852**, 234–243 (1986)
55. N. Gerasimchuk, T. Maher, P. Durham, K.V. Domasevitch, J. Wilking, A. Mokhir, Inorg. Chem. **46**, 7268–7284 (2007)
56. S. Shahzadi, S. Ali, K. Shahid, M. Yousaf, S.K. Sharma, K. Qanungo, J. Chin. Chem. Soc. **57**, 659–670 (2010)
57. J. Zhang, P.L. Yang, N.S. Gray, Nat. Rev. Cancer **9**, 28–39 (2009)
58. S. Shahzadi, K. Shahid, S. Ali, M. Mazhar, K. Khan, J. Iran. Chem. Soc. **2**, 277–288 (2005)